



Published in final edited form as:

J Nutr Biochem. 2021 March ; 89: 108580. doi:10.1016/j.jnutbio.2020.108580.

White Button Mushroom (*Agaricus bisporus*) Disrupts Androgen Receptor Signaling in Human Prostate Cancer Cells and Patient-Derived Xenograft

Xiaoqiang WANG¹, Desiree Ha¹, Hitomi Mori¹, Shiuan Chen^{1,*}

¹Department of Cancer Biology, City of Hope, 1500 E. Duarte Rd., Duarte, CA 91010, USA

Abstract

White button mushroom (WBM) (*Agaricus bisporus*) is a potential prostate cancer (PCa) chemopreventative and therapeutic agent. Our clinical phase I trial of WBM powder in patients with biochemically recurrent PCa indicated that WBM intake reduced the circulating levels of prostate-specific antigen (PSA). We hypothesized that WBM exerts its effects on PCa through the androgen receptor (AR) signaling axis. Therefore, we conducted a reverse translational study with androgen-dependent PCa cell lines (LNCaP and VCaP) and patient-derived-xenografts (PDX) from a prostate tumor (TM00298). In both LNCaP and VCaP cells, western blots and qRT-PCR assays indicated that WBM extract (6~30 mg/mL) suppressed DHT-induced PSA expression and cell proliferation in a dose-dependent manner. Immunofluorescence analysis of AR revealed that WBM extract interrupted the AR nuclear-cytoplasmic distribution. PSA promoter-luciferase assay suggested that WBM extract inhibited DHT-induced luciferase activity. RNA-Seq on WBM-treated LNCaP cells confirmed that WBM treatment suppressed the androgen response pathways and cell-cycle control pathways. Our PDX showed that oral intake of WBM extract (200 mg/kg/day) suppressed tumor growth and decreased PSA levels in both tumors and serum. In the present study, we also identified a conjugated linoleic acid isomer (CLA-9Z11E) as a strong AR antagonist by performing LanthaScreen™ TR-FRET AR Coactivator Interaction Assays. The inhibitory effect of CLA-9Z11E (IC50: 350 nM) was nearly two times stronger than the known AR antagonist, cyproterone acetate (IC50: 672 nM). The information gained from this study improves the overall understanding of how WBM may contribute to the prevention and treatment of PCa.

*Correspondence to: Shiuan Chen Ph.D.; Department of Cancer Biology, City of Hope, 1500 E. Duarte Rd., Duarte, CA 91010, USA. Phone: +1-626-256-4673; schen@coh.org.

⁶Author Contribution

XQ and SC designed the experiments, analyzed the results, and wrote the manuscript. XQ, DH, HM performed the experiments.

Publisher's Disclaimer: This is a PDF file of an unedited manuscript that has been accepted for publication. As a service to our customers we are providing this early version of the manuscript. The manuscript will undergo copyediting, typesetting, and review of the resulting proof before it is published in its final form. Please note that during the production process errors may be discovered which could affect the content, and all legal disclaimers that apply to the journal pertain.

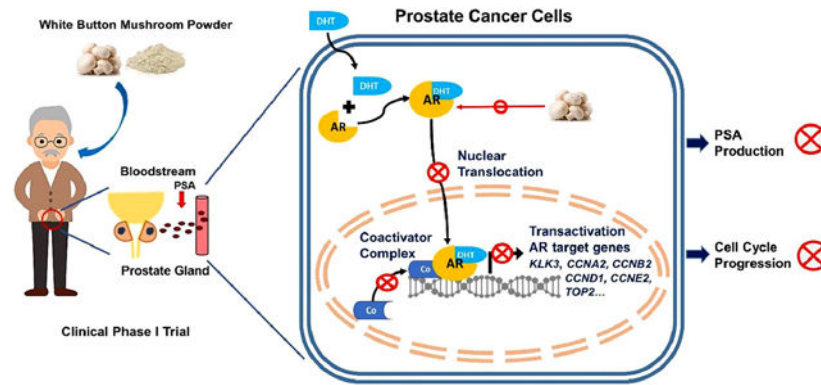
^{5.1}Ethics Approval and Consent

Experiments performed in this study comply with current laws in the United States of America. All applicable institutional guidelines for the care and use of animals were followed. Animal research procedures were approved by the Institutional Animal Care and Use Committee (IACUC) at City of Hope (IACUC-15091). Facilities are credited by AAALAC (Association for Assessment and Accreditation of Laboratory Animal Care) and operated according to NIH guidelines.

^{5.2}Conflict of Interest

The authors declare that they have no conflict of interest.

Graphical Abstract



Keywords

White Button Mushroom; Conjugated (9Z, 11E)-Linoleic Acid; Androgen Receptor; Prostate-Specific Antigen; Cell Cycle; Prostate Cancer

1, Introduction

Prostate cancer (PCa) is the second most frequent cancer and the fifth leading cause of cancer death in men worldwide [1]. Almost all PCas begin in an androgen-dependent state, where androgens and androgen receptor (AR) signaling are the hallmarks of oncogenesis and disease progression because they promote PCa cell proliferation and survival [2]. Thus, for primary local treatment, androgen deprivation therapy (ADT) is usually used as the first line of treatment [3]. This approach has been successful in achieving tumor regression and reduction in the tumor marker, prostate specific antigen (PSA). Even with ADT, approximately 35% of patients eventually develop a rise in PSA, and a smaller proportion go on to develop metastatic disease. These recurrent cancers cannot be cured and since treatment options are limited, ADT is continued in most cases [4]. However, the associated side effects of ADT are potentially significant, and the benefits for asymptomatic patients are unclear. For these patients, an intervention with minimal toxicities needs to be developed [5].

Both epidemiological [6] and clinical studies [7, 8] suggest that fungi-derived molecules may play a significant role in PCa prevention, reducing the risk of recurrence, and therapy. In many cultures, fungi are used medicinally in traditional herbal medicine. Several mushroom species have been shown to exhibit anticancer effects both *in vitro* and *in vivo*, including triggering cytostatic and/or cytotoxic effects in prostate, colon, and breast cancer [9]. White button mushroom (WBM, *Agaricus bisporus*) is the most common and budget-friendly, edible mushroom in North America. Our laboratory pioneered the preclinical and clinical studies of WBM on both breast cancer and prostate cancer. [7, 10~12]. We have shown that WBM extract significantly inhibits PCa cell growth by inducing cytotoxicity both *in vitro* and *in vivo* [12]. Based on the preclinical observations, our team at City of Hope conducted the first single-arm clinical phase I trial of WBM

powder in 36 patients with biochemically recurrent PCa. In this trial, we evaluated the feasibility, toxicity, and biological activity of prolonged therapy with WBM powder. Two patients exhibited a complete response, with a reduction of PSA to undetectable levels, and two other patients experienced partial clinical and PSA responses. Thirteen patients had some reduction in PSA from the baseline. However, in the patients with a significant or modest PSA reduction, serum testosterone levels remained in the non-castrated range. PSA decrease was not correlated with changes in serum androgens, such as testosterone, dihydrotestosterone (DHT), or dehydroepiandrosterone (DHEA). These findings indicated that therapy with WBM appears to impact PSA levels without interfering with pre-receptor steroidogenesis [7].

Serum PSA is a marker used to assist in the initial and recurrent diagnosis of PCa [13]. It also serves as a surrogate endpoint marker for pharmacological strategies, such as ADT [14]. PSA is expressed and secreted by normal, hyperplastic, and cancerous prostatic epithelia. PSA has been extensively studied as a model androgen-responsive gene because within the enhancer and promoter region of the PSA gene, there are both strong consensus androgen-responsive elements (AREs) and weak non-consensus AREs. The synergistic binding of androgen-bound AR to those regions likely accounts for its typical and strong androgen-dependent transactivation [15]. Thus, the consistently expressed and secreted PSA in PCa reflects AR transcriptional activity in cancer cells. The decline in PSA levels, in response to therapeutic agents, is caused either by tumor cell death or by decreasing AR-stimulated PSA production in surviving tumor cells [16].

The objective of the present study was to investigate the mechanism of WBM extract on PSA production in androgen-dependent tumor cells. We conducted this bedside-to-bench reverse translational study to confirm our clinical trial observations at both the *in vitro* and *in vivo* levels. Androgen-dependent PCa cell lines (LNCaP and VCaP) [17] and a patient-derived-xenograft (PDX) tumor with AR and PSA expression (TM00298) [18] were used.

2, Materials and Methods

2.1 Production of Mushroom Extract

The mushroom extract was prepared via hot water extraction as previously described [12]. Briefly, 6 g of freeze-dried WBM powder was boiled in 1L hot water for 3 hours. The broth was centrifuged at 3000 g for 30 minutes, twice, to collect the fraction of supernatant. The liquid fraction was rotor-evaporated to dryness and then re-dissolved in 1 mL of hot water to produce a 6X mushroom extract. Therefore, the concentration of 6X WBM extract originated from 6 g dried WBM powder/mL (6 mg/ μ L). 60 g of fresh mushrooms can generate 6 g of dried WBM powder.

2.2 Cell Culture and Chemical Regents

Androgen-dependent PCa cell lines (LNCaP and VCaP), an androgen-independent PCa cell line (PC3), and a human non-cancerous prostate cell line (RWPE-1) were obtained from the American Type Culture Collection (ATCC). LNCaP, VCaP, and PC3 cells were maintained

in ATCC-formulated Dulbecco's Modified Eagle's Medium/DMEM (ATCC, Rockville, MD) with 10% fetal bovine serum (FBS, Omega Scientific, Tarzana, CA) and 1% penicillin/streptomycin (Fisher Scientific, Chino, CA) at 37°C with 5% CO₂. RWPE-1 was grown in keratinocyte serum-free medium with bovine pituitary extract and human recombinant epidermal growth factor (Fisher Scientific, Chino, CA) at 37°C with 5% CO₂. The genetic integrity of these cell lines was confirmed by DNA fingerprinting short-tandem repeat (STR) analysis at City of Hope's Integrative Genomic Core.

For the *in vitro* experiments, cells were grown in DMEM with 10% charcoal-dextran stripped FBS (Omega Scientific, Tarzana, CA) with WBM extract or chemical reagents. DHT (>99% pure, Sigma Aldrich, St. Louis, MO), enzalutamide (Enza) (Selleckchem, Houston, TX), and conjugated (9Z,11E) linoleic acid (CLA-9Z11E) (Sigma Aldrich, St. Louis, MO) were applied at the concentrations indicated in our studies as described below.

2.3 Cell Viability and Cell Proliferation Assay

Cells were cultured in hormone-deprived medium for two days and then seeded at 3×10^3 cells/100 μ L in a 96-well plate. 24 hours post-seeding, the cells were treated with different concentrations of mushroom extract (1 μ L/mL~20 μ L/mL) [12] or enzalutamide (5 μ M) supplied with or without 1 nM DHT, as seen in typical, physiological concentrations in older men [19]. Cell viability was measured by CellTiter 96® AQueous MTS Reagent (Promega, Madison, WI), which determined the reduction of the MTS tetrazolium compound by metabolically active cells. Cell proliferation was measured by CyQuant NF Cell Proliferation reagent (Thermo-Fisher, Grand Island, NY), which determined the cellular DNA content.

2.4 Western Blot Analysis

Cells were treated as indicated conditions for 48h and harvested to extract total cellular protein with RIPA Buffer (Abcam, Cambridge, MA). Protein concentration was quantified by BCA Protein Assay Kit (Thermo-Fisher, Grand Island, NY) and resolved in 10% SDS-PAGE, and then transferred onto a PVDF blotting membrane (Amersham Bioscience, Marlborough, MA). Primary antibodies of AR (D6F11), PSA (D6B1), Bcl-2 (D55G8), Bcl-xl (54H6), Bax (D2E11), Cleaved Caspase-3 (5A1E), GAPDH (14C10), Nucleolin (D4C7O) (Cell Signaling Technology, Danvers, MA), and HRP-conjugated secondary anti-rabbit antibody (Sigma Aldrich, St. Louis, MO) were used at their recommended concentrations by their respective manufacturers.

2.5 Quantitative Real-time PCR

Total RNA was extracted from cultured cells using the RNeasy Mini kit (QIAGEN, Germantown, Maryland) and then used to synthesize complementary DNA (cDNA) with SuperScript IV VILO Master Mix (Thermo-Fisher, Grand Island, NY). qPCR was performed using CFX Connect Real-Time System (Bio-Rad, Hercules, California) with PerfeCTa SYBR Green FastMix (Quantabio, Beverly, Massachusetts). The primers used in the qPCR were obtained from Primer Bank (<https://pga.mgh.harvard.edu/primerbank>). The target gene messenger RNA (mRNA) level was normalized to GAPDH expression.

2.6 Nuclear-cytoplasmic Separation

Cells were treated as indicated conditions for 48h. The cytoplasmic and nuclear fractions were obtained using the Nuclear Extract Kit (Active Motif, Carlsbad, CA) according to the manufacturer's protocol. The AR expression levels in cytoplasmic and nuclear fractions were detected and quantified by western blot analysis.

2.7 Immunofluorescence Staining

Cells were grown on Lab-Tek[®] Chamber Slide (Sigma Aldrich, St. Louis, MO). After the indicated treatment for 48h, cells were fixed in pre-chilled acetone/methanol (1:1) and rehydrated with PBS. The slide was blocked with Antibody Diluent (Agilent, S302283-2), then incubated with an anti-AR antibody (D6F11, Cell Signaling Technology, Danvers, MA), followed by incubation with the secondary antibody Mach 2 Rabbit HRP-polymer diluted 1:2 (Biocare Medical, RHRP520L) in Van Gogh Diluent (Biocare Medical, PD902L). Tyramine Signal Amplification (TSA) fluorophores were used as the substrate to the HRP-conjugated antibody (FP1497001KT, Perkin-Elmer, San Jose, California). Slides were mounted using VECTASHIELD[®] Antifade Mounting Media with DAPI (Vector, Burlingame, CA). Representative images were captured at 20X and 100X, with scale bar of 100 μ m and 20 μ m, respectively, on EVOS[™] FL Auto Imaging System.

2.8 AR Reporter Luciferase Assay

The cells were transiently co-transfected with an androgen-dependent PSA promoter-firefly luciferase reporter plasmid (50 ng) and pRL-TK-Luciferase plasmid (50 ng) using XtremeGENE[™] HP DNA Transfection Reagent (Sigma Aldrich, St. Louis, MO). Then, they were treated by indicated concentrations of WBM extract, enzalutamide, or CLA-9Z11E, with or without DHT supplementation (1 nM). The Dual-Luciferase Assay Kit (Promega, Madison, WI) was used to measure luciferase activity, which was read using a microplate luminometer (Molecular Device, San Jose, CA). Readings were normalized to *Renilla* luciferase activity by a pRL-TK-Luciferase plasmid. PSA promoter-firefly luciferase reporter plasmid was obtained from Dr. Jeremy Jones at Beckman Research Institute of City of Hope [20].

2.9 Androgen Receptor Coactivator Screen Assay

Through gas chromatography analysis, we previously identified a conjugated linoleic acid isomer 9Z, 11E (CLA-9Z11E) as an active component in WBM extract (an average of 45.7% of the total fatty acid from WBM) [11] and showed that CLA-9Z11E inhibited LNCaP cell proliferation in a dose-dependent manner [12]. To measure the potency of CLA-9Z11E against AR, we conducted Thermo-Fisher LanthaScreen[™] TR-FRET Nuclear Receptor Coregulator Interaction Assays, which determined the ligand dose-dependency for the recruitment of coregulator peptides to nuclear receptor. Ten-point titrations ranging from 5 nM to 100 μ M were applied to generate a dose-response curve in both the agonist and antagonist models. A more detailed protocol can be found on the Thermo-Fisher website.

2.10 Total PSA Measurement

Cell culture media and/or serum samples from animal experiments were collected to detect total PSA concentration. Total PSA (human) ELISA kit (Enzo, Farmingdale, NY) was applied according to the manufacturer's protocol.

2.11 RNA-Seq and Data Analysis

LNCaP cells were treated by 1 nM DHT, with or without WBM extract (3 $\mu\text{L}/\text{mL}$), for 48h. Total RNA was extracted from three sets of treated cells using the RNeasy Mini kit (QIAGEN, Germantown, Maryland). Total RNA extract was sequenced by the Integrative Genomics Core at City of Hope. RNA-Seq raw data was submitted to Gene Expression Omnibus (GEO) with a GEO accession number of GSE160723. Gene Set Enrichment Analysis (GSEA) was used to process sequencing, map sequence reads, and analyze systems-level pathways. KEGG-pathway was generated by Pathview Web [21]

To evaluate the androgen-responsive genes affected by mushroom treatment, the RNA-Seq dataset derived from mushroom extract (3 $\mu\text{L}/\text{mL}$, 48h)-treated LNCaP cells was cross-analyzed with the other two transcriptional datasets, which were generated from DHT (1 nM, 48h)-treated LNCaP cells [22] and enzalutamide (10 μM , 48h)-treated LNCaP cells [23]. Datasets were downloaded from GEO. The overlapping genes from these three datasets were displayed using a Venn diagram from Venny ^{2.1}.

2.12 Animal Experiments

PCa patient-derived xenograft/PDX tumor (TM00298) (The Jackson Laboratory Sacramento, CA) was a primary prostatic adenocarcinoma from a 71-year old patient, which was characterized as an androgen-responsive tumor by strong AR expression and enzalutamide responsiveness [18]. Tumor fragments (3 mm^3) were subcutaneously implanted into 6~8-week-old recipient NSG male intact mice (average body weight of 30 g). Tumor volumes averaged 400 mm^3 after 30 days. The mice were randomly divided into 3 groups (2 mice in control (Ctrl), 2 mice in enzalutamide (Enza), and 5 mice in 6X mushroom (WBM)) with indicated treatments for 6 days. The Ctrl group was gavaged with 100 μL PBS with 1% carboxymethyl cellulose daily, while the other two groups were gavaged with 300 $\mu\text{g}/\text{mice}/\text{day}$ enzalutamide (at a dose of 10 mg/kg) or 6 $\text{mg}/\text{mice}/\text{day}$ 6X mushroom extract (at a dose of 200 $\text{mg}/\text{kg}/\text{day}$) in 100 μL PBS with 1% carboxymethyl cellulose, respectively. Tumor volume was recorded daily. Body weight was monitored daily as an indicator of the mice's overall health. At the end of 6 days of treatment, mice were euthanized and their blood samples were collected. Xenograft tumors were removed, weighed, and stored for RNA extraction or histological analysis. Liver, kidney, and reproductive organs (prostate gland and testes) were also collected to assess target organ toxicity.

Eight-week-old male intact C57BL mice (The Jackson Laboratory, Sacramento, CA) were used for the evaluation of WBM-mediated toxicity *in vivo*. The mice were randomly divided into 3 groups (3 mice in Ctrl, 3 mice in Enza, and 4 mice in WBM) with the same treatments as performed on the PDX tumor-implanted NSG mice. The analyses included body/organ

weight measurements, histological analyses of the prostate glands, and quantification of hepatotoxic/nephrotoxic markers, as well as a skeletal muscle marker.

2.13 Immunohistochemistry and Histopathological Analysis

Hematoxylin and eosin (H&E) staining and immunohistochemistry (IHC) on formalin-fixed tumor tissues were performed by the Pathology Core at City of Hope. Antibodies used in IHC included: AR (SP107, Sigma-Aldrich), PSA (M0750, DAKO), p63 (M7317, DAKO), and Ki-67 (MIB-1, DAKO). Slides were reviewed first at 10X magnification to identify areas of positive staining, followed by confirmation and quantification at 20X magnification. IHC staining was scored by QuPath software (version 0.2). The immunoreactivity of AR was reported as H score (0~300) by combining the nuclear proportion score (percentage of positive cells) and the intensity of staining (none/0, mild/1, moderate/2, and strong/3). Ki67 and PSA were reported by their percentage of positive cells. Representative images were acquired at magnifications of 10X, 20X, and 40X with scale bar of 400 μ m, 200 μ m, and 100 μ m, respectively, using an Olympus BX46 microscope with a DP27 camera.

2.14 Statistical Methods and Data Analysis

Results are shown as means \pm standard deviation (SD). All statistical analyses were performed using GraphPad Prism software (version 8.0). The significance of the differences between mean values was determined by multiple Student's *t*-tests. P-values <0.05 (* p<0.05, **p<0.01, ***p<0.001) were considered statistically significant and all tests were two-tailed. Benjamini and Hochberg's method was used to compute the adjusted p-value and control the false discovery rate (FDR) for RNA-Seq analysis.

3. Results

3.1 WBM Extract Decreases AR Expression and PSA Production in Androgen-dependent PCa Cells

The objective of the present study was to investigate the mechanism of WBM extract on AR-dependent PSA production in viable tumor cells. Our previous study reported that WBM extract induced apoptosis in PCa cells (LNCaP and PC3) at a concentration of 20 μ L/mL [12]. Thus, we performed a cell viability assay and checked for apoptosis markers on LNCaP, VCaP, PC3, and RWPE-1 cells at varying concentrations of WBM extract (1~20 μ L/mL) for 48h, with or without DHT supplementation (1 nM). The results showed that at a high concentration (20 μ L/mL), WBM exhibited a cytotoxic effect on all PCa cell lines, except for the human non-cancerous prostate cell line (RWPE-1) (Supplementary Figure 1A and 1B). However, at low concentrations (1~5 μ L/mL), androgen-dependent PCa cell lines (LNCaP and VCaP) were more sensitive to WBM when DHT was present (Supplementary Figure 1A). The western blot from LNCaP cells further indicated that in the presence of DHT and at a concentration of 10 μ L/mL of WBM, anti-apoptotic markers (Bcl-2/XL) significantly decreased and, the pro-apoptotic marker (Bax) and cleaved-caspases 3 increased. (Supplementary Figure 1C). We interpreted that WBM exhibited mild cytotoxicity at a low dose (1~5 μ L/mL) in androgen-responsive PCa cells.

LNCaP and VCaP cells were then treated with WBM extract (1~5 $\mu\text{L}/\text{mL}$) or enzalutamide (5 μM) in the presence of DHT (1 nM). The results showed that WBM extract induced a dose-dependent, anti-proliferative effect by decreasing cellular DNA content (Figures 1A and 1B) and secreted PSA levels (Figures 1C and 1D). The latter results were confirmed at the protein level by western blot (Figures 1E and 1F) and at the gene expression level by qRT-PCR (Figures 1G and 1H). The cellular level of AR (mRNA and protein) was also evaluated in both cell lines under WBM treatment. The results indicated that the cellular level of AR was reduced in both LNCaP cells (Figures 1E and 1G) and VCaP cells, with a stronger effect in VCaP cells (Figures 1F and 1H).

3.2 WBM Extract Interrupts AR Nuclear-cytoplasmic Distribution and Transactivation in Androgen-dependent PCa Cells

Nuclear-cytoplasmic relocation is an important prerequisite for activated AR to enter the nucleus and bind to multiple AREs [24]. Thus, the effect of WBM on AR nuclear-cytoplasmic distribution was assessed by immunofluorescence. As shown in Figure 2A (LNCaP) and Figure 2B (VCaP), AR was found predominantly in the nucleus of DHT-treated cells. While on the contrary, in the absence of DHT, the majority of AR was present in the cytosol of the cells [24]. However, when cells were treated with both DHT and WBM extract, the nuclear localization of AR was reduced in a dose-responsive manner. Enzalutamide, an AR antagonist which is known to inhibit DHT binding to the AR, nuclear translocation of the AR, DNA binding, and coactivator recruitment [25], was used as a reference control (Figures 2A and 2B).

To confirm the above patterns of the subcellular distribution of the AR, the nuclear and cytoplasmic fractions of LNCaP (Figure 2C) and VCaP (Figure 2E) cells were analyzed by western blot. WBM treatment resulted in a reduction of AR protein both in the nuclear and cytoplasmic fractions for both cell lines. However, AR levels in the nuclear fractions decreased more than those in the cytoplasmic fractions following WBM treatment. These results agree with the observations made by immunofluorescence staining.

Relocation of AR into the nucleus leads to transactivation via AREs. To examine the effect of WBM on DHT-induced AR transactivation [26], LNCaP (Figure 2D) and VCaP (Figure 2F) cells were transfected with PSA promoter-luciferase reporter plasmid which contained AREs in the promoter region. While DHT (1 nM), alone, significantly induced luciferase activity, such induction was inhibited by WBM extract in a dose-dependent manner, suggesting that WBM extract inhibited DHT-induced AR transactivation. As a reference control, the luciferase activity did not change when we performed an ARE reporter assay on LNCaP and VCaP cells with WBM alone (without DHT supplement) (Supplementary Figure 2A and 2B). This confirmed that treatment of WBM extract alone does not affect the luciferase activity and that the chemical(s) in WBM extract behave as AR antagonist(s). With these findings, we conclude that WBM extract treatment interrupts AR expression, nuclear-cytoplasmic distribution, and transactivation in androgen-dependent PCa cells.

3.3 WBM Extract Suppresses the Expression of AR Responsive Genes

To confirm the antagonistic effects of WBM extract on AR signaling, LNCaP cells were treated with 1 nM DHT, with or without WBM extract (3 μ L/mL), for 48h in triplicates, and total RNA was isolated and sequenced (Supplementary Figure 3A). There were 155 up-regulated genes (Fold-change ≥ 2 , $p < 0.05$) versus 185 down-regulated genes (Fold-change ≤ 0.5 , $p < 0.05$). The clustering of differentially expressed genes was visualized using a heat map (Figure 3A). Among them, *KLK3* (the gene encode PSA) was ranked as the most down-regulated gene (down-regulated 2.6 folds by WBM extract versus without WBM extract) (Supplementary Figure 3B). To identify the key pathways related to WBM treatment, GSEA-Hallmarks analysis was performed on the differentially expressed genes. As shown in Figure 3B, the most significantly down-regulated pathways were related to androgen response and cell proliferation (hallmarks of E2F target, G2M checkpoint, and mitotic spindle formation). Such observations were cross-validated by the GSEA-KEGG analysis. As shown in Supplementary Figure 3C, WBM treatment suppressed cell cycle division genes including: cyclins, cell division cycles, origin recognition complex (ORC), and mini-chromosome maintenance (MCM). On the other hand, WBM up-regulated genes were associated with the P53 pathway, apoptosis, xenobiotic metabolism, as well as immune function regulated pathways, such as reactive oxygen species and TNF α -NF κ B pathway (Figure 3B).

We further evaluated these regulated genes by performing a Venn Diagram Analysis that showed the overlapping genes in WBM-treated LNCaP (3 μ L/mL WBM with 1 nM DHT, 48h), DHT-treated LNCaP (1 nM DHT, 48h, GSE11428), and enzalutamide-treated LNCaP (10 μ M enzalutamide with 1 nM DHT, 48h, GSE110905) (Figure 3C). As shown in Figure 3D, there were 39 common genes among the 3 datasets. The GSEA-Hallmark analysis on those genes indicated that the most significant hallmarks were cell-cycle control pathways and androgen response pathways. To validate the RNA-Seq results generated from LNCaP cells treated with WBM, the expression levels of several androgen-regulated genes (from the 39 common genes in Figure 3D; *PSA*, *CCNA2*, *CCNB2*, *CCND1*, *CCNE2*, *TOP2*) were measured in LNCaP and VCaP cells (Figure 3E and F) by qRT-PCR. Those genes were effectively down-regulated in the presence of WBM extract.

3.4 CLA-9Z11E in WBM Extract Inhibits AR Coactivator Interaction and PSA Expression

We previously identified CLA-9Z11E as an active component in WBM extract [11]. It inhibited LNCaP cell proliferation in a dose-dependent manner [12]. Thermo-Fisher LanthaScreenTM TR-FRET Nuclear Receptor Coregulator Interaction Assays revealed that CLA-9Z11E exerted a strong antagonist potency against the recruitment of an AR coactivator peptide to the AR (Figure 4A). The inhibitory effect of CLA-9Z11E (IC₅₀: 350 nM) was nearly two times stronger than the known AR antagonist, cyproterone acetate (IC₅₀: 672 nM). CLA-9Z11E did not exhibit AR agonist activity (Figure 4B).

To confirm the antagonist potency of CLA-9Z11E to attenuate DHT-induced transcriptional activity of the AR, a PSA promoter-luciferase reporter assay was performed. PSA promoter-luciferase reporter plasmid was transfected into LNCaP (Figure 4C) and VCaP (Figure 4D) cells, followed by treatment with different concentrations of CLA-9Z11E (10~500 μ M).

The DHT-induced luciferase activity was interrupted by CLA-9Z11E in a dose-dependent manner. The inhibitory effects of CLA-9Z11E on AR and PSA expression were measured in both LNCaP (Figure 4E) and VCaP (Figure 4F) cells using qRT-PCR. The mRNA of PSA was repressed in the presence of CLA-9Z11E, further confirming the antagonist potency of CLA-9Z11E to attenuate DHT-induced PSA expression, while the levels of AR mRNA were maintained. These results indicate that CLA-9Z11E is an active molecule that can down-regulate AR activity. Considering the hydrophobic property of CLA-9Z11E, higher concentrations of CLA-9Z11E were needed in cell culture studies than in the direct binding assays using AR protein (Figure 4A).

3.5 WBM Extract Suppresses PDX Tumor Growth and PSA Expression

Our *in vitro* studies suggested that WBM affects the AR signaling axis. TM00298 is a PDX model characterized as an androgen-responsive tumor by strong expression of AR, PSA, and responsiveness to enzalutamide [18]. We used this mouse model to examine the effects of WBM extract (Figure 5A). We observed the trend that oral intake of WBM extract or enzalutamide suppressed tumor growth (Figure 5B) and weight (Figure 5C), as compared to our control. Serum PSA declined in WBM or enzalutamide-treated mice (Figure 5E). This observation was further confirmed at the PSA protein level by IHC (Figure 5D) and at the gene expression level by qRT-PCR (Figure 5F). However, AR expression (H-Score) in tumors was not affected by WBM (Figures 5D and 5F). We learned from the *in vitro* studies that WBM also exerts anti-proliferative potency. The expression of Ki67 and DNA topoisomerase 2 α (TOP2A), an enzyme that controls the topologic states of DNA during transcription, was strongly suppressed by WBM or enzalutamide. (Figure 5D and 5F).

More importantly, the weight of the prostate gland under WBM treatment slightly decreased when compared to the prostate glands in either the control or enzalutamide-treated mice (Figure 5G). A follow-up histological study indicated that WBM treatment induced prostatic acinar atrophy by reducing the size and number of AR-positive complex acini in the anterior region of the prostate gland (Figure 5H). The complex acini were composed of columnar epithelial cells and displayed typical cribriform or papillary partners in the anterior part of a normal prostate gland [27]. When we evaluated the WBM treatment-induced prostate glandular atrophy in C57BL mice, we observed a similar histological change, as seen previously in the NSG mice (Supplementary Figure 5A). In benign human prostate glands, enzalutamide has been reported to induce glandular atrophy with ruptured atrophic acini, and prominent basal cells, after long-term exposure [28]. Such observations were also reported in rat, dog, and mice under long-term (4~16 weeks) enzalutamide intake [29]. Our findings on mushroom extract, in conjunction with other researchers on enzalutamide, support that the *in vivo* activity of mushroom chemicals resembles enzalutamide. In addition, we evaluated the basal cells (p63⁺) in the atrophic glands of C57BL mice by IHC. Due to the acinar atrophy, we observed an overall decrease in the number of p63 positive basal cells. Although this reduction does not define atrophic changes, it provides insight on the compositional changes within the complex acini. (Supplementary Figure 5B).

The body weights and major organs' weights (liver, kidney, testes) (Supplementary Figure 4A~D) did not change in WBM-treated NSG mice. To further determine whether the intake

of mushroom extract causes severe organ toxicity, we performed additional experiments using C57BL mice with WBM treatment, identical to the experiments on NSG mice. Our results indicated that WBM extract did not exert generalized organ toxicity. As shown in Supplementary Figure 4E–F, overall body weight and skeletal muscle weight did not change upon WBM or enzalutamide treatment for 12 days in C57BL mice. We isolated the skeletal muscle from C57BL mice and checked the expression level of insulin growth factor-1 (IGF1), an AR targeting gene that regulates skeletal muscle growth [30]. Enzalutamide suppressed IGF1 expression in skeletal muscle, while WBM displayed mild suppression on IGF1 (Supplementary Figure 4G). We collected fresh livers and kidneys and checked for hepatotoxic markers (aspartate aminotransferase/AST and alanine aminotransferase/ALT) [31] and nephrotoxic markers (kidney injury molecule-1/KIM-1) [32] by qRT-PCR. As shown in Supplementary Figure 4H, the results revealed that WBM did not exhibit hepatotoxicity and nephrotoxicity. Our previous clinical phase I trial, that evaluated the potential toxicity of WBM in humans, revealed minimal side effects that included hepatotoxicity and muscle pain, most of which were limited to grade 1 classification [7].

4. Discussion

Our clinical phase I trial indicated that in patients with biochemically recurrent PCa, intake of WBM affects PSA levels without correlation to the levels of circulating androgens [7]. We hypothesized that WBM extract and its active molecules therein act on PSA expression through the AR signaling axis. In this reverse translational study, we used androgen-dependent PCa cell lines, LNCaP and VCaP, as *in vitro* models, which express AR and PSA, both at the mRNA and protein levels [17]. Meanwhile, the TM00298 PDX was used as an *in vivo* model [18], which has a strong expression on the AR signaling pathway and clinical reflection. Traditionally, preclinical PCa *in vivo* models were generated by cell line-derived xenografts [33]. Recently, PDX models are the replacements for overcoming limitations associated with cell lines and for obtaining a more accurate reflection of clinical responses in patients [34]. Enzalutamide is used to treat PCa and acts by inhibiting AR signaling at multiple steps in the pathway [25]. Thus, enzalutamide was used in our experiments as a reference control for the responsiveness of AR signaling. The decline in PSA levels in response to therapeutic agents is caused either by tumor cell death or by decreasing AR-stimulated PSA production in surviving tumor cells [16]. The objective of the present study was to investigate the mechanism of WBM extract on AR-induced PSA production in viable tumor cells.

Our previous study has reported that WBM extract induced DNA fragmentation and apoptosis in PCa cells (LNCaP and PC3) at a high concentration [12]. We learned that the decline in PSA levels in response to therapeutic agents was caused either by tumor cell death or by decreasing AR-stimulated PSA production in surviving tumor cells [14, 16]. One objective of the present study was to investigate the mechanism of WBM extract on AR-induced PSA production in viable tumor cells. To determine the dose range of WBM for the *in vitro* study, we performed a MTS cell viability assay and checked for apoptosis markers. As shown in Supplementary Figure 1A and B, for androgen-dependent PCa Cells (LNCaP and VCaP), cell viability started to decline at 5 μ L/mL in the

presence of DHT. The western blot from LNCaP cells (Supplementary Figure 1C) also indicated that in the presence of DHT and at a concentration of 10 $\mu\text{L}/\text{mL}$ of WBM, anti-apoptotic markers (Bcl-2/XL) significantly decreased and, the pro-apoptotic marker (Bax) and cleaved-caspases 3 increased. Therefore, our *in vitro* experiments were performed at a low concentration (1~5 $\mu\text{L}/\text{mL}$) such that WBM displayed mild apoptotic effects on the androgen-dependent PCa cells.

The present study also demonstrated that WBM induced a dose-dependent, anti-proliferative effect at a low concentration range (1~5 $\mu\text{L}/\text{mL}$) that maintained viable cells (Figure 1A and B). Results from RNA-Seq further supported the anti-proliferative phenotype that the most significantly down-regulated pathways by WBM were related to cell proliferation and cell cycle division (hallmarks of E2F target, G2M checkpoint, and mitotic spindle formation). The transcription of key genes related to cell cycle division and DNA replication, named as *CCNA2*, *CCNB2*, *CCND1*, *CCNE2*, *TOP2*, were measured by qRT-PCR in both LNCaP and VCaP cells (Figure 3). *In vivo* studies with our PDX model also illustrated that oral intake of WBM extract suppressed tumor growth by inhibiting cell proliferation, as measured by Ki67 with IHC and *TOP2* gene expression by qRT-PCR. AR acts as a master regulator of cell cycle transition by directly controlling multiple gatekeepers in G1-S and G2-M phases [35]. Androgen directly induces the expression of cyclin D via Rb-E2F axis in early G1 events [36] and regulates the assembly of the pre-replication complex (pre-RC) by origin recognition complex (ORC), cell division cycle 6 homolog (Cdc6), and minichromosome maintenance (MCM) in the middle G1 phase [37]. Thus, acting as a licensing factor for DNA replication in the S phase [38]. In contrast to D-type cyclins, cyclin E, cyclin A, and cyclin B were also regulated by AR, which triggered mitotic exit and completion of the cell cycle [39]. Interestingly, as shown in Supplementary Figure 3C, WBM suppressed cell cycle division genes including different types of cyclins, cell division cycles, ORC, and MCM. Collectively, these results confirm that WBM extract affects PCa by interrupting AR-dependent cell cycle division and DNA replication. Moreover, research has discovered that cell cycle feedback may regulate AR activity, either at the transcriptional or post-transcriptional level, because the AR locus is under Rb/E2F1 control. Suppression of E2F1 would lead to the deregulation of AR expression [35, 39]. Such regulation may explain our observation that WBM extract suppressed AR expression at the transcriptional levels in VCaP cells (Figure 1H). Indeed, the AR level in VCaP is higher than in other PCa cell lines, including LNCaP. Therefore, VCaP cells may respond more sensitively towards anti-androgen agents than other cell lines [40].

We previously identified CLA-9Z11E by gas chromatography analysis as an active component in WBM extract [11] and showed that CLA-9Z11E inhibited LNCaP cell proliferation in a dose-dependent manner [12]. Others have also reported in LNCaP cells that CLA-9Z11E exhibited potent anti-androgenic effects by suppressing PSA expression [41]. In the present study, we extended these studies by performing LanthaScreen™ TR-FRET AR Coactivator Interaction Assays for a direct interaction of CLA-9Z11E with AR. TR-FRET-based assays were developed using the LanthaScreen™ panel of fluorescein-labeled coregulator peptides to investigate conformational changes of AR upon ligand binding, either by determining the affinity of the ligand-bound receptor for different coregulator peptides or by identifying additional agonists or antagonists via displacement

or recruitment of a specific coregulator peptide [42]. We report here that CLA-9Z11E exerts a strong antagonist potency against AR coactivator via direct protein-protein interaction assay (Figure 4). Even though the IC₅₀ of CLA-9Z11E towards AR-coactivator interaction was determined to be as low as 350 nM, the biological effective dose in cells was as high as 100 μM [12, 41]. Cellular intake and transport of long-chain fatty acids across cellular membranes do not occur by simple diffusion, but rather by membrane protein associated translocases. Thus, it may require a high supply concentration to reach the desired intracellular aqueous concentration [43]. CLA has shown various health-promoting benefits including anti-oxidation, anti-inflammation, anti-carcinogenesis, et al [44]. Some CLA isomers have been identified to exert anti-cancer potency such as CLA-9Z11E and CLA-10E12Z [45, 46]. To our best knowledge, this is the first direct biochemical evidence of CLA-9Z11E that demonstrates its antagonist potency against AR. We further confirmed the antagonist potency of CLA-9Z11E by AR reporter luciferase assay and *PSA* expression by qRT-PCR; all those results support that CLA-9Z11E can act as an AR antagonist. However, in considering that WBM extract is a mixture of multiple components, we cannot rule out the possibility that additional chemicals beside CLA-9Z11E in WBM extract may potentially deregulate AR activity at different levels.

For the *in vivo* study, we fed 6X WBM extract at a dose of the extract originating from 200 mg WBM powder/kg/day (average body weight of mice is 30 g, equal to 6 mg/mice/day). The 6X WBM extract was originated from 6 g freeze-dried WBM powder in 1mL water (6mg/μL). Oral intake of WBM extract (200 mg/kg/day) significantly suppressed the growth of the PDX tumor, with declined levels of serum and tissue PSA. The expression of Ki67 and DNA topoisomerase 2α (TOP2A) was also strongly suppressed by WBM (Figure 5). For adult men with an average body weight of 80 kg, the estimated daily WBM powder intake would be 16 g/day. In our clinical phase I trial, we examined 6 dosages of WBM powder pellet, beginning with 4 g/d to 14 g/d [11].

In terms of the concentration of CLA-9Z11E in WBM extract, our previous study, via GS-MS analysis, identified CLA-9Z11E in active WBM fractions as an average of 45.7% of total fatty acid [12]. The inhibitory concentration of CLA-9Z11E on AR activity in LNCaP and VCaP cells is above 100 μM, equal to 28.045 mg/L (MW of CLA-9Z11E is 280.45 g/M). It has been estimated that the lipid content in WBM is 0.34 g/100 g [47], equal to 2 μg lipid content/6 mg powder (generated from 60 mg WBM). For the *in vitro* study, 1 μL/mL of 6X WBM extract contains 6 mg of dry WBM. Therefore, an extract from 6 mg dry WBM powder was used in our *in vitro* experiment. While it is difficult to directly quantify how much CLA-9Z11E is present in 2 μg of lipid, we can assume that its level would be much lower than 28 μg. Such analysis suggests that additional chemicals in WBM can suppress AR activity, and that they have yet to be defined.

In conclusion, through carefully designed *in vitro* and *in vivo* experiments, we showed that WBM intake affects PCa by interfering with the AR signaling axis. We also showed the antagonistic effect of the WBM component, CLA-9Z11E. The information gained from this study improves the overall understanding of how WBM may contribute to the prevention and treatment of PCa and serves as an important scientific basis for a phase 2 clinical trial using WBM on PCa.

Supplementary Material

Refer to Web version on PubMed Central for supplementary material.

Acknowledgments

This work was supported by NIH CA227230 (Chen). We thank the City of Hope Integrative Genomics Core, Pathology Research Services Core and Small Animal Studies Core, which are supported by the National Cancer Institute of the National Institutes of Health under award number P30CA033572, for their excellent technical support. We acknowledged Dr. Hyun-Jeong Shim for her advice on animal study and Dr. David Sadava for his critical reading of the manuscript.

Abbreviations

AR	androgen receptor
ADT	androgen deprivation therapy
ARE	androgen response element
ATCC	American Type Culture Collection
CCNA2	Cyclin A2
CCNB2	Cyclin B2
CCND1	Cyclin D1
CCNE2	Cyclin E2
CLA-9Z11E	conjugated (9Z, 11E)-linoleic acid
Ctrl	control
DHT	dihydrotestosterone
DHEA	dehydroepiandrosterone
DMEM	Dulbecco's Modified Eagle's Medium
Enza	enzalutamide
FDR	false discovery rate
H&E	hematoxylin and eosin
IHC	immunohistochemistry
IF	immunofluorescence
GEO	Gene Expression Omnibus
GSEA	Gene Set Enrichment Analysis
KEGG	Kyoto Encyclopedia of Genes and Genomes
MCM	mini-chromosome maintenance

ORC	origin recognition complex
PCa	Prostate Cancer
PSA	prostate-specific antigens
PDXs	patient-derived xenografts
RNA-Seq	RNA Sequencing
STR	short-tandem repeat
TOP2A	DNA topoisomerase 2 α
WBM	white button mushroom

8. References

- 1). Bray F, Ferlay J, Soerjomataram I, Siegel RL, Torre LA, Jemal A. Global cancer statistics 2018: GLOBOCAN estimates of incidence and mortality worldwide for 36 cancers in 185 countries. *CA Cancer J Clin.* 2018.68(6):394–424. [PubMed: 30207593]
- 2). Schweizer MT, Yu EY. AR-Signaling in Human Malignancies: Prostate Cancer and Beyond. *Cancers (Basel).* 2017. 9(1). PII: E7. [PubMed: 28085048]
- 3). Cannata DH, Kirschenbaum A, Levine AC. Androgen deprivation therapy as primary treatment for prostate cancer. *J Clin Endocrinol Meta.* 2012. 97(2):360–365.
- 4). Chang AJ, Autio KA, Roach M 3rd, Scher HI. “High-Risk” Prostate Cancer: Classification and Therapy. *Nat Rev Clin Oncol* 2014.11(6): 308–323. [PubMed: 24840073]
- 5). Artibani W, Porcaro AB, De Marco V, Cerruto MA, Siracusano S. Management of Biochemical Recurrence after Primary Curative Treatment for Prostate Cancer: A Review. *Urol Int.* 2018. 100(3):251–262. [PubMed: 29161715]
- 6). Zhang S, Sugawara Y, Chen S, Beelman RB, Tsuzuki T, Tomata Y, Matsuyama S, Tsuji I. Mushroom consumption and incident risk of Prostate Cancer in Japan: A pooled analysis of the Miyagi Cohort Study and the Ohsaki Cohort Study. *Int J Cancer.* 2020.146(10):2712–2720. [PubMed: 31486077]
- 7). Twardowski P, Kanaya N, Frankel P, Synod T, Ruel C, Pal SK, Junqueira M, Prajapati M, Moore T, Tryon P, Chen S. A phase I trial of mushroom powder in patients with biochemically recurrent prostate cancer: Roles of cytokines and myeloid-derived suppressor cells for *Agaricus bisporus*-induced prostate-specific antigen responses. *Cancer.* 2015.121(17):2942–50. [PubMed: 25989179]
- 8). Davidson KT, Zhu Z, Fang Y. Phytochemicals in the Fight against Cancer. *Pathol Oncol Res.* 2016 22(4):655–60. [PubMed: 26857640]
- 9). Lee JW, Lee WB, Kim W, Min BI, Lee H, Cho SH. Traditional herbal medicine for cancer pain: a systematic review and meta-analysis. *Complement Ther Med.* 2015.23(2):265–74. [PubMed: 25847565]
- 10). Grube BJ, Eng ET, Kao YC, Kwon A, Chen S. White button mushroom phytochemicals inhibit aromatase activity and breast cancer cell proliferation. *J Nutr.* 2001.131(12):3288–9. [PubMed: 11739882]
- 11). Chen S, Oh SR, Phung S, Hur G, Ye JJ, Kwok SL, Shrode GE, Belury M, Adams LS, Williams D. Anti-aromatase activity of phytochemicals in white button mushrooms (*Agaricus bisporus*). *Cancer Res.* 2006 12 15;66(24):12026–34. [PubMed: 17178902]
- 12). Adams LS, Phung S, Wu X, Ki L, Chen S. White button mushroom (*Agaricus bisporus*) exhibits anti-proliferative and pro-apoptotic properties and inhibits prostate tumor growth in athymic mice. *Nutr Cancer.* 2008.60(6):744–56. [PubMed: 19005974]
- 13). Albertsen PC. Prostate Cancer screening with prostate-specific antigen: Where are we going? *Cancer.* 2018.124(3):453–455. [PubMed: 29231972]

- 14). Tannock IF. Can modeling of PSA dynamics accelerate drug development for prostate cancer? *Lancet Oncol.* 2017.18(1):16–18. [PubMed: 27979601]
- 15). Balk SP, Ko YJ, Bubley GJ. Biology of prostate-specific antigen. *J Clin Oncol.* 2003.21(2):383–91. [PubMed: 12525533]
- 16). Dixon SC, Knopf KB, Figg WD. The control of prostate-specific antigen expression and gene regulation by pharmacological agents. *Pharmacol Rev.* 2001.53(1):73–91. [PubMed: 11171939]
- 17). Sampson N, Neuwirt H, Puhr M, Klocker H, Eder IE. In vitro model systems to study androgen receptor signaling in prostate cancer. *Endocr Relat Cancer.* 2013.20(2): R49–64. [PubMed: 23447570]
- 18). Sekhar Konjeti R., Wang Jian, Freeman Michael L., Kirschner Austin N.. Radiosensitization by enzalutamide for human prostate cancer is mediated through the DNA damage repair pathway. *PLoS One.* 2019.14(4): e0214670. [PubMed: 30933998]
- 19). Nawata H, Kato K, Obayashi H. Age-dependent change of serum 5alpha-dihydrotestosterone and its relation to testosterone in man. *Endocrinol Jpn.* 1977. 24(1):41–5. [PubMed: 862570]
- 20). Jones JO, An WF, Diamond MI. AR Inhibitors identified by high throughput microscopy detection of conformational change and subcellular localization. *ACS Chem Biol.* 2009. 20; 4(3): 199–208.
- 21). Luo W, Pant G, Bhavnasi YK, Blanchard SG Jr, Brouwer C. Pathview Web: user friendly pathway visualization and data integration. *Nucleic Acids Res.* 2017. 3; 45(W1):W501–W508. [PubMed: 28482075]
- 22). Wang Q, Li W, Zhang Y, Yuan X et al. Androgen receptor regulates a distinct transcription program in androgen-independent prostate cancer. *Cell* 2009.138(2):245–56. [PubMed: 19632176]
- 23). Zhang Y, Pitchiaya S, Cie lik M, Niknafs YS et al. Analysis of the androgen receptor-regulated lncRNA landscape identifies a role for ARLNC1 in Prostate Cancer progression. *Nat Genet* 2018. 50(6):814–824. [PubMed: 29808028]
- 24). Saranyutanon S, Srivastava SK, Pai S, Singh S, Singh AP. Therapies Targeted to Androgen Receptor Signaling Axis in Prostate Cancer: Progress, Challenges, and Hope. *Cancers (Basel).* 2019.12(1). PII: E51. [PubMed: 31877956]
- 25). Ito Y, Sadar MD. Enzalutamide and blocking androgen receptor in advanced prostate cancer: lessons learned from the history of drug development of antiandrogens. *Res Rep Urol.* 2018.16; 10:23–32. [PubMed: 29497605]
- 26). Lee DK, Chang C. Endocrine mechanisms of disease: Expression and degradation of androgen receptor: mechanism and clinical implication. *J Clin Endocrinol Metab.* 2003. 88(9):4043–54. [PubMed: 12970260]
- 27). Oliveira DS, Dzinic S, Bonfil AI, Saliganan AD, Sheng S, Bonfil RD. The mouse prostate: a basic anatomical and histological guideline. *Bosn J Basic Med Sci.* 2016.10; 16(1):8–13. [PubMed: 26773172]
- 28). Ning YM, Pierce W, Maher VE, Karuri S, Tang SH, Chiu HJ, Palmby T, Zirkelbach JF, Marathe D, Mehrotra N, Liu Q, Ghosh D, Cottrell CL, Leighton J, Sridhara R, Ibrahim A, Justice R, Pazdur R. Enzalutamide for treatment of patients with metastatic castration-resistant prostate cancer who have previously received docetaxel: U.S. Food and Drug Administration drug approval summary. *Clin Cancer Res.* 2013. 15;19 (22):6067–73. [PubMed: 24141628]
- 29). Evans AJ. Treatment effects in prostate cancer. *Mod Pathol.* 2018. 31(S1):S110–121. [PubMed: 29297495]
- 30). Yin L, Lu L, Lin X et al. Crucial role of androgen receptor in resistance and endurance trainings-induced muscle hypertrophy through IGF-1/IGF-1R- PI3K/Akt- mTOR pathway. *Nutr Metab (Lond)* 2020. 17, 26. [PubMed: 32256674]
- 31). Meunier L, Larrey D. Drug-Induced Liver Injury: Biomarkers, Requirements, Candidates, and Validation. *Front Pharmacol.* 2019. 11; 10:1482. [PubMed: 31920666]
- 32). Griffin BR, Faubel S, Edelstein CL. Biomarkers of Drug-Induced Kidney Toxicity. *Ther Drug Monit.* 2019. 41(2):213–226. [PubMed: 30883514]
- 33). Cunningham D, You Z. In Vitro and in Vivo Model Systems Used in Prostate Cancer Research. *J Biol Methods.* 2015. 2(1):e17. [PubMed: 26146646]

- 34). Namekawa T, Ikeda K, Horie-Inoue K, Inoue S. Application of Prostate Cancer Models for Preclinical Study: Advantages and Limitations of Cell Lines, Patient-Derived Xenografts, and Three-Dimensional Culture of Patient-Derived Cells. *Cells*. 2019. 20; 8(1):74.
- 35). Balk SP, Knudsen KE. AR, the cell cycle, and prostate cancer. *Nucl Recept Signal*. 2008; 6: e001. [PubMed: 18301781]
- 36). Murthy S, Wu M, Bai VU, Hou Z, Menon M, Barrack ER, Kim SH, Reddy GP. Role of Androgen Receptor in the Progression of LNCaP Prostate Cancer Cells from G1 to S Phase. *PLoS One*. 2013. 8(2):e56692. [PubMed: 23437213]
- 37). D'Antonio JM, Vander Griend DJ, Isaacs JT. DNA licensing as a novel androgen receptor-mediated therapeutic target for prostate cancer. *Endocr Relat Cancer*. 2009. 16(2): 325–332. [PubMed: 19240183]
- 38). Litvinov IV, Vander Griend DJ, Antony L, Dalrymple S, De Marzo AM, Drake CG, Isaacs JT. Androgen Receptor as a Licensing Factor for DNA Replication in Androgen-Sensitive Prostate Cancer Cells. *Proc Natl Acad Sci USA*. 2006. 103(41):15085–90. [PubMed: 17015840]
- 39). Schiewer MJ, Augello MA, Knudsen KE. The AR Dependent Cell Cycle: Mechanisms and Cancer Relevance. *Mol Cell Endocrinol*. 2012. 352(1-2):34–45. [PubMed: 21782001]
- 40). Cai C, He HH, Chen S, Coleman I, Wang H, Fang Z, Chen S, Nelson PS, Liu XS, Brown M, Balk SP. Androgen Receptor Gene Expression in Prostate Cancer is Directly Suppressed by the Androgen Receptor through Recruitment of Lysine Specific Demethylase 1. *Cancer Cell*. 2011. 18; 20(4): 457–471. [PubMed: 22014572]
- 41). Gasmi J, Sanderson JT. Growth inhibitory, antiandrogenic, and pro-apoptotic effects of puniic acid in LNCaP human Prostate Cancer Cells. *J Agric Food Chem*. 2010.58(23):12149–56. [PubMed: 21067181]
- 42). Carazo A, Pávek P. The Use of the LanthaScreen TR-FRET CAR Coactivator Assay in the Characterization of Constitutive Androstane Receptor (CAR) Inverse Agonists. *Sensors (Basel)* 2015. 15(4): 9265–9276. [PubMed: 25905697]
- 43). Pohl J, Ring A, Ehehalt R, Herrmann T, Stremmel W. New Concepts of Cellular Fatty Acid Uptake: Role of Fatty Acid Transport Proteins and Caveolae. *Proc Nutr Soc*. 2004. 63(2):259–62. [PubMed: 15294040]
- 44). Den Hartigh LJ. Conjugated Linoleic Acid Effects on Cancer, Obesity, and Atherosclerosis: A Review of Pre-Clinical and Human Trials with Current Perspectives. *Nutrients*. 2019.11; 11(2). PII: E370. [PubMed: 30754681]
- 45). Kelley NS, Hubbard NE, Erickson KL. Conjugated linoleic acid isomers and cancer. *J Nutr*. 2007.137(12):2599–607. [PubMed: 18029471]
- 46). Dhar Dubey KK, Sharma G, Kumar A. Conjugated Linolenic Acids: Implication in Cancer. *J Agric Food Chem*. 2019.67(22):6091–6101. [PubMed: 31070027]
- 47). Feeney MJ, Dwyer J, Hasler-Lewis CM, Milner JA, Noakes M, Rowe S, Wach M, Beelman RB, Caldwell J, Cantorna MT, Castlebury LA, Chang ST, Cheskin LJ, Clemens R, Drescher G, Fulgoni VL 3rd, Haytowitz DB, Hubbard VS, Law D, Myrdal Miller A, Minor B, Percival SS, Riscuta G, Schneeman B, Thornsby S, Toner CD, Woteki CE, Wu D. Mushrooms and Health Summit proceedings. *J Nutr*. 2014. 144(7):1128S–36S. [PubMed: 24812070]

Highlights

- White button mushroom (WBM) extract inhibits androgen receptor (AR) activity
- WBM extract suppresses androgen responsive genes' expression and androgen dependent cell cycle progression
- WBM intake suppresses AR positive patient derived xenograft (PDX) prostatic tumor growth in mice
- Conjugated-Linoleic Acid isomer (CLA-9Z11E) is an active component in WBM that acts as an AR antagonist

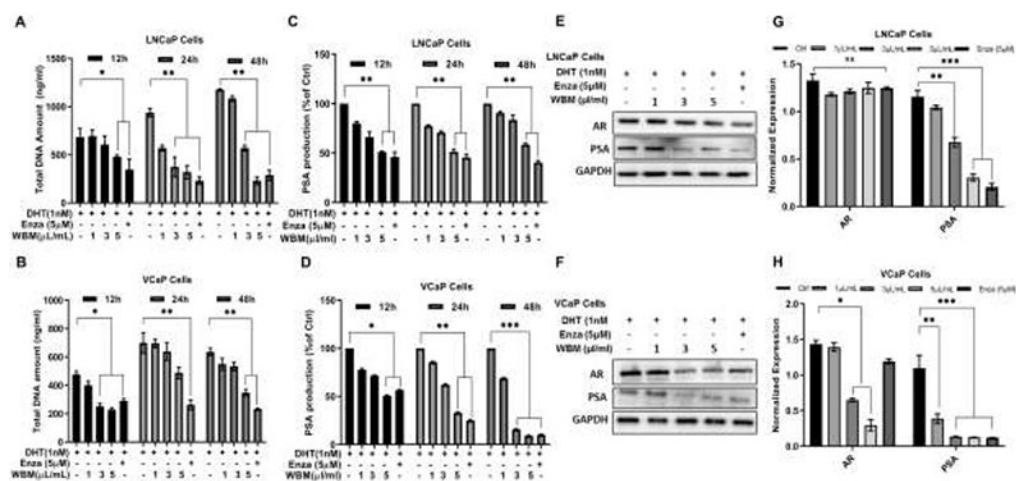


Figure 1. WBM extract causes a dose-dependent decrease in cell proliferation, cellular AR, and PSA levels.

Cells were treated with the mushroom extract (WBM, 1 μ L/mL~5 μ L/mL) or enzalutamide (Enza, 5 μ M) supplied with 1 nM DH for 12~48h. The proliferation of **A**) LNCaP and **B**) VCaP cells was measured by the CyQuant NF Cell Proliferation reagent. The PSA production in the culture medium of **C**) LNCaP and **D**) VCaP cells was detected by PSA (human) ELISA kit. Total protein of AR and PSA in **E**) LNCaP and **F**) VCaP cells was detected by western blot, and mRNA of AR and PSA in **G**) LNCaP and **H**) VCaP cells was quantified by qRT-PCR. The results are mean \pm standard deviation of three independent experiments, p values were determined by multiple Student's *t*-tests. **p*<0.05, ***p*<0.01, ****p*<0.001. ns. No significant difference.

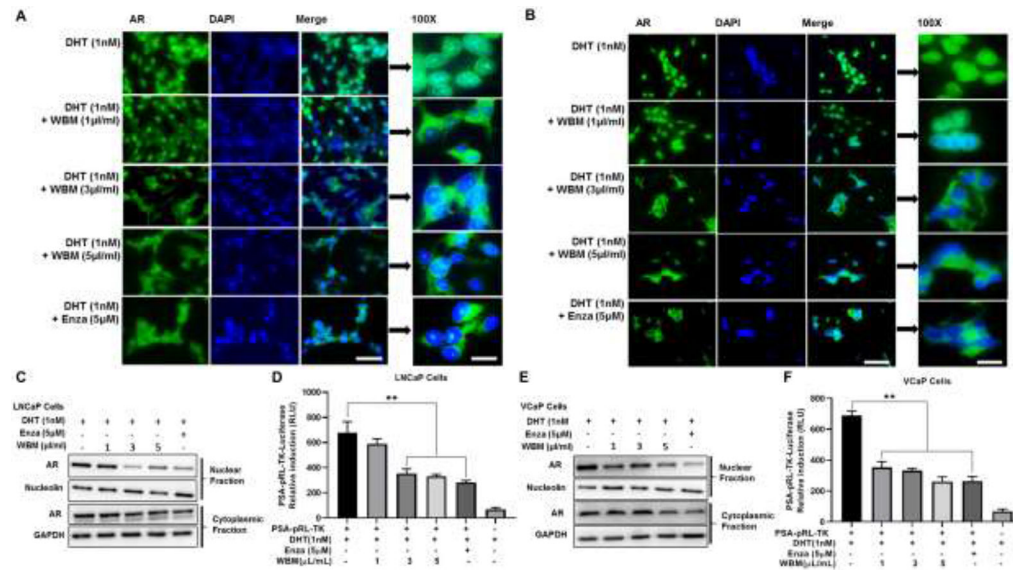


Figure 2. WBM extract interrupts AR expression, AR nuclear-cytoplasmic distribution, and transactivation.

Cells were treated with the mushroom extract (WBM, 1 $\mu\text{L}/\text{mL}$ ~5 $\mu\text{L}/\text{mL}$) or enzalutamide (Enza, 5 μM) supplied with 1 nM DHT for 48h. The AR cellular localization in **A**) LNCaP and **B**) VCaP cells was determined by immunofluorescence staining. Magnification at 20X and 100X with a scale bar of 100 μm and 20 μm , respectively. The protein amount of AR in the cytoplasmic and nuclear fractions of **C**) LNCaP and **E**) VCaP cells was determined by western blot. GAPDH and nucleolin were used as the cytoplasmic and nuclear loading controls, respectively. The AR reporter activity in **D**) LNCaP and **F**) VCaP cells was determined by PSA promoter-Luciferase assay. ** $p < 0.01$. ns. No significant difference.

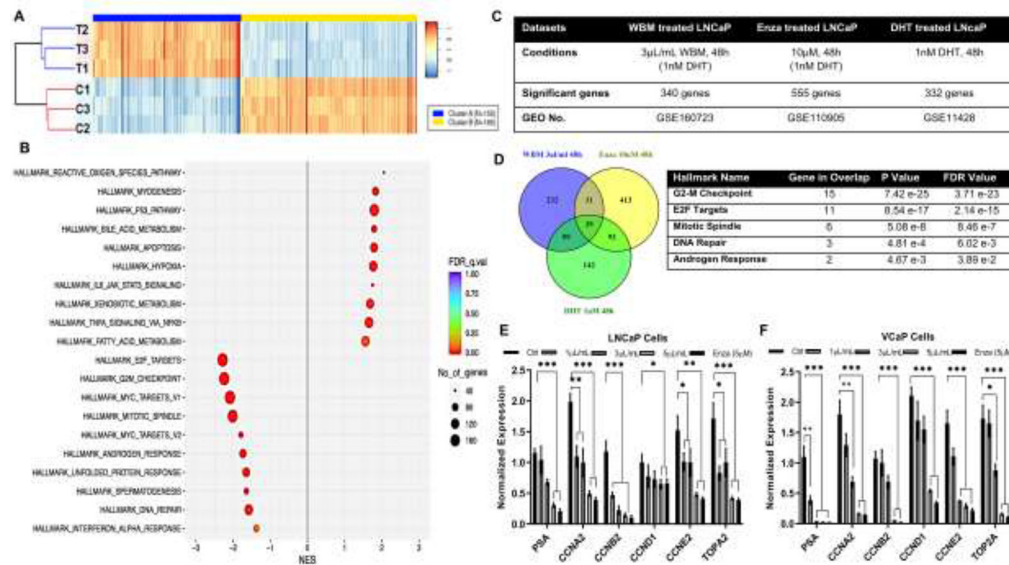


Figure 3. WBM extract suppresses the expression of AR responsive genes.

LNCaP cells were treated with 1 nM DHT, with or without 6X mushroom extract (3 μ L/mL), for 48h. Total RNA was sequenced. **A**) Significant regulated genes between Ctrl (1 nM DHT, 3 samples) versus Treatment (1 nM DHT and WBM extract, 3 samples) were demonstrated by a heat map. There were 155 up-regulated genes (Cluster A, Fold-change 2, $p < 0.05$) versus 185 down-regulated genes (Cluster B, Fold-change 0.5, $p < 0.05$). **B**) Identification of pathways was analyzed by Gene Set Enrichment Analysis (GSEA) with hallmarks of datasets. False discovery rate (FDR) was < 0.01 , Number of significant genes (NES) > 40 . **C**) Three RNA-Seq datasets derived from LNCaP cells with treatments of mushroom extract (3 μ L/mL WBM with 1 nM DHT, 48h), enzalutamide (10 μ M Enza with 1 nM DHT, 48h,) and DHT (1 nM DHT, 48h) were applied to enrich AR responsive genes. **D**) Venn Diagram Analysis demonstrated the distribution of the number of genes in three datasets. There were 39 common genes among 3 datasets. Top 5 GSEA-Hallmarks of 39 genes ($p < 0.05$, $FDR < 0.25$). Key Genes involved in Top5 hallmarks were quantified by qRT-PCR in LNCaP **E**) and VCaP **F**) cells.

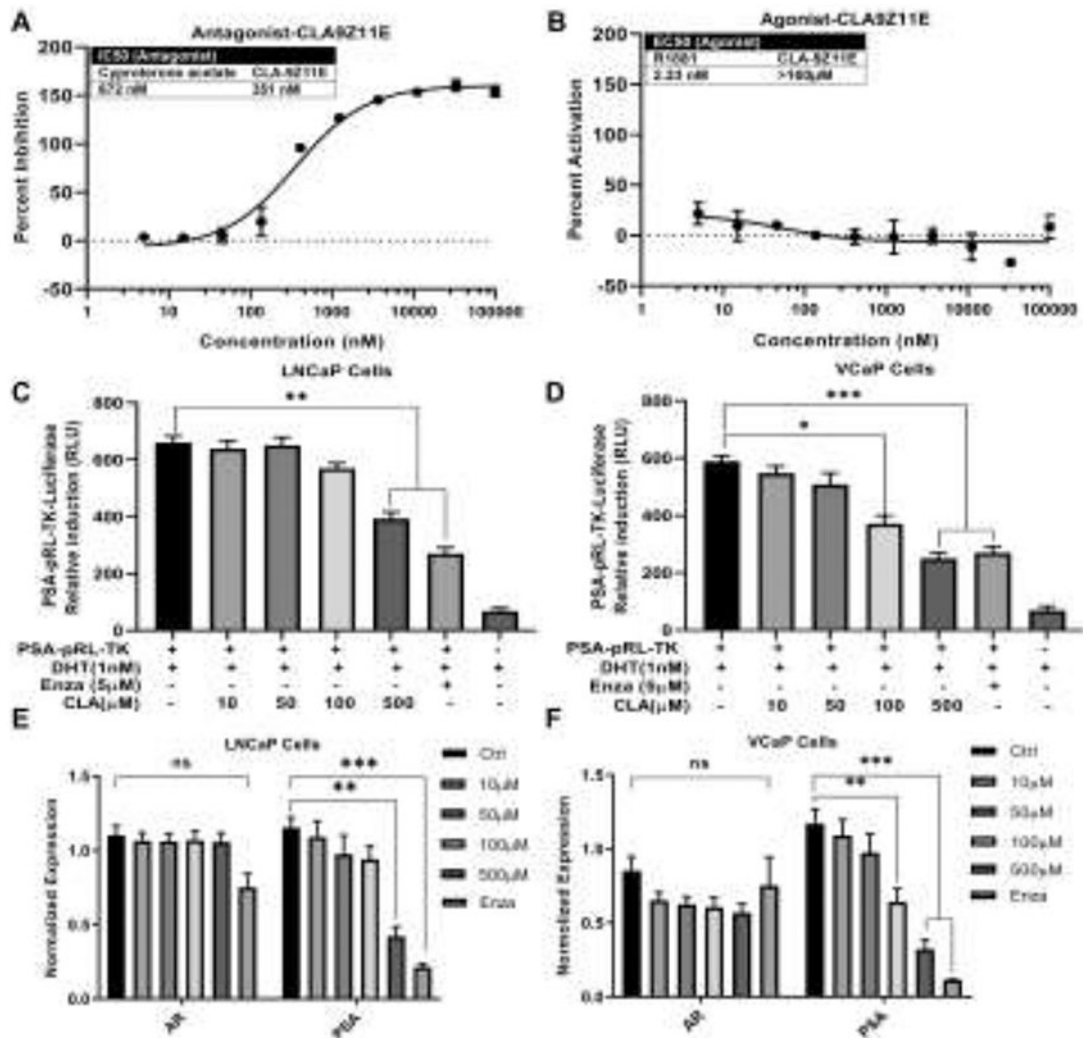


Figure 4. CLA-9Z11E inhibits AR coactivator interaction and PSA expression.

AR Coactivator Interaction Assay in **A**) antagonist and **B**) agonist models were performed to test the ability of CLA-9Z11E to affect coactivator peptide recruitment and binding to AR. Cyproterone acetate (IC₅₀: 672 nM) was used as a positive control for the antagonist assay and R1881, a synthetic AR agonist, was used for the agonist assay. Data are expressed as mean ± standard deviation of duplicate assays. LNCaP and VCaP cells were treated by 1 nM DHT with CLA-9Z11E (10 μM~500 μM) for 48h. AR reporter activity in **C**) LNCaP and **D**) VCaP cells was determined by PSA promoter-luciferase assay. The mRNA levels of AR and PSA in **E**) LNCaP and **F**) VCaP cells was quantified by qRT-PCR. The results are expressed as mean ± standard deviation of three independent experiments, p values were determined by multiple Student's t-tests. *p<0.05, **p<0.01, ***p<0.001. ns. No significant difference.

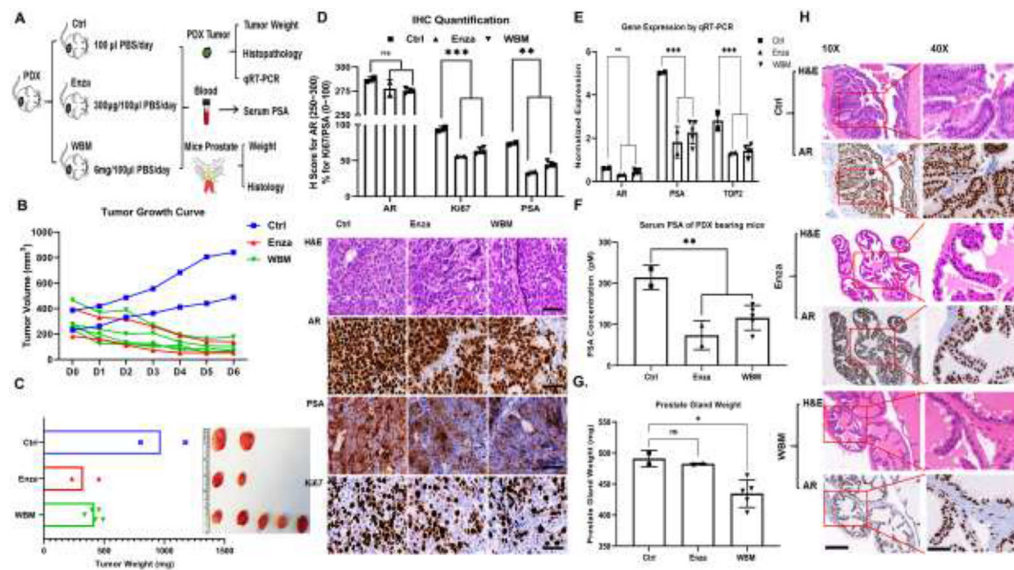


Figure 5. Intake of WBM extract suppresses PDX tumor growth and PSA expression.

A) Male 6~8-week-old NSG mice bearing PCa PDX fragments were gavaged with WBM extract (6 mg/mice/day, 5 mice in WBM group), enzalutamide (300 µg/mice/day, 2 mice in Enza group) or PBS (2 mice in Ctrl group) for 6 days. **B)** The tumor volume in mm³ is represented by individual values in each group by different colors. **C)** Tumor xenografts in each group are illustrated and tumor weights are represented by individual values in each group by different colors. **D)** Hematoxylin and eosin (H&E) and immunohistochemistry (IHC) staining of AR, PSA, and Ki67 on formalin-fixed tumor tissues in each group. The IHC staining was scored (upper panel) by the QuPath software (version 0.2). Immunoreactivity of AR was reported as H score (upper left panel). Ki67 and PSA were reported by their percentage of positive cells (upper right panels). Scale bar of representative images is 40X by 100 µm. **E)** The mRNA level of *AR*, *PSA*, and *TOP2* in tumor fragments of each group was quantified by qRT-PCR. **F)** The PSA concentrations in serum were detected by PSA (human) ELISA kit. **G)** The prostate gland weight in each group is presented as a median±standard error for the mean. **H)** Hematoxylin and eosin (H&E) and immunohistochemistry (IHC) of AR staining on the formalin-fixed prostate gland in each group. The AR-positive complex acini in anterior prostate gland are shown. Scale bar for 10X and 40X, with scale bar of 400 µm and 100 µm, respectively. p values were determined by multiple Student's t-tests. *p<0.05, **p<0.01, ***p<0.001. ns. No significant difference.